Synthesis of Cobalt-, Nickel-, Copper-, and Zinc-Based, Water-Stable, Pillared Metal-Organic Frameworks

ARTICLE *in* LANGMUIR · OCTOBER 2014

Impact Factor: 4.46 · DOI: 10.1021/la503269f · Source: PubMed

5 AUTHORS, INCLUDING:

Himanshu Jasuja
Georgia Institute of Technology
16 PUBLICATIONS **481** CITATIONS
SEE PROFILE

Nicholas Burtch
Georgia Institute of Technology
8 PUBLICATIONS **136** CITATIONS
SEE PROFILE

Langmuir

Article

pubs.acs.org/Langmuir

Synthesis of Cobalt-, Nickel-, Copper-, and Zinc-Based, Water-Stable, Pillared Metal−Organic Frameworks

Himanshu Jasuja, Yang Jiao, Nicholas C. Burtch, You-gui Huang, and Krista S. Walton*

School of Chemical and Biomolecular Engineering, Georgia Institute of Technology, 311 Ferst Drive Northwest, Atlanta, Georgia 30332, United States

Supporting Information

ABSTRACT: The performance of metal−organic frameworks (MOFs) in humid or aqueous environments is a topic of great significance for a variety of applications ranging from adsorption separations to gas storage. While a number of water-stable MOFs have emerged recently in the literature, the majority of MOFs are known to have poor water stability compared to zeolites and activated carbons, and there is therefore a critical need to perform systematic water-stability studies and characterize MOFs comprehensively after water exposure. Using these studies we can isolate the specific factors governing the structural stability of MOFs and direct the future synthesis efforts toward the construction of new, water-stable MOFs. In this work, we have extended our previous work on the systematic water-stability studies of MOFs and synthesized new, cobalt-, nickel-, copper-, and zinc-based, water-stable, pillared MOFs by incorporating structural factors such as ligand sterics and catenation into the framework. Stability is assessed by using water vapor adsorption isotherms along with powder X-ray diffraction patterns and results from BET modeling of N_2 adsorption isotherms before and after water exposure. As expected, our study demonstrates that unlike the parent DMOF structures (based on Co, Ni, Cu, and Zn metals), which all collapse under 60% relative humidity (RH), their corresponding tetramethyl-functionalized variations (DMOF-TM) are remarkably stable, even when adsorbing more than 20 mmol of H_2O/g of MOF at 80% RH. This behavior is due to steric factors provided by the methyl groups grafted on the BDC (benzenedicarboxylic acid) ligand, as shown previously for the Zn-based DMOF-TM. Moreover, 4,4′,4″,4‴-benzene-1,2,4,5-tetrayltetrabenzoic acid based, pillared MOFs (based on Co and Zn metals) are also found to be stable after 90% RH exposure, even when the basicity of the bipyridyl-based pillar ligand is low. This is due to the presence of catenation in their frameworks, similar to MOF-508 (Zn-BDC-BPY), which has also been reported to be stable after exposure to 90% RH.

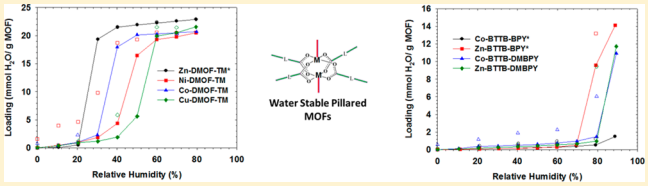

1. INTRODUCTION

Metal−organic frameworks (MOFs) are constructed by the self-assembly of organic ligands and metal-containing nodes.[1] MOFs have garnered much attention in a variety of fields related to porous materials, such as sensing,[1,2] adsorption-based gas storage,[1−7] gas separation,[1,2,5,7−10] catalysis,[1−3,5,7,11] and drug delivery.[1,2,11] This is due to their record-breaking values of surface area and pore volume, facile pore tunability, and almost infinite set of structure possibilities with diverse topologies. While a number of water-stable MOFs have recently been synthesized in the literature, many MOFs exhibit poor stability under humid and aqueous conditions that restrict their potential use in industrial applications, such as air purification, CO_2 capture, and catalysis.[12] Thermodynamically, water being a more basic ligand (pK_a ∼15.7), it can often displace the less basic organic ligands (typically carboxylates) coordinated to the metal centers and, hence, can breakdown the framework.

Despite the significance of this issue, the literature consists of relatively few systematic water-stability studies for MOFs.[13−29] Moreover, the prevailing literature is rather scattered in the type of water exposure conditions, and the particular characterization techniques used to quantify the water stability of MOFs experimentally vary significantly among publications. In most of the studies reported,[30−48] MOFs are exposed to ambient air in the lab or soaked in liquid water, but water adsorption isotherms are rarely reported, and postexposure powder X-ray diffraction (PXRD) alone is widely used to characterize MOFs. PXRD is a simple technique that provides information about the long-range crystallinity of the structure, though it is not capable of detecting short-range surface collapse. Hence, it is a qualitative technique and not a comprehensive way to characterize MOFs after water exposure. This has led to misleading conclusions about the water stability of MOFs. For example, Jasuja and Walton[19] and Liu et al.[44] reported contrasting observations about the stability of MOF-508 (Zn-BDC-BPY), with the former highlighting the need for surface area analysis in addition to PXRD to reach a conclusion with a higher confidence level.

Overall, it has been seen that the strength of the bond between the metal centers and the ligand is a strong indicator of the MOF hydrothermal stability.[16] Carboxylate-ligand-based MOFs, such as MOF-5 and UMCM-1, are highly unstable

Received: August 19, 2014
Revised: October 15, 2014
Published: October 17, 2014

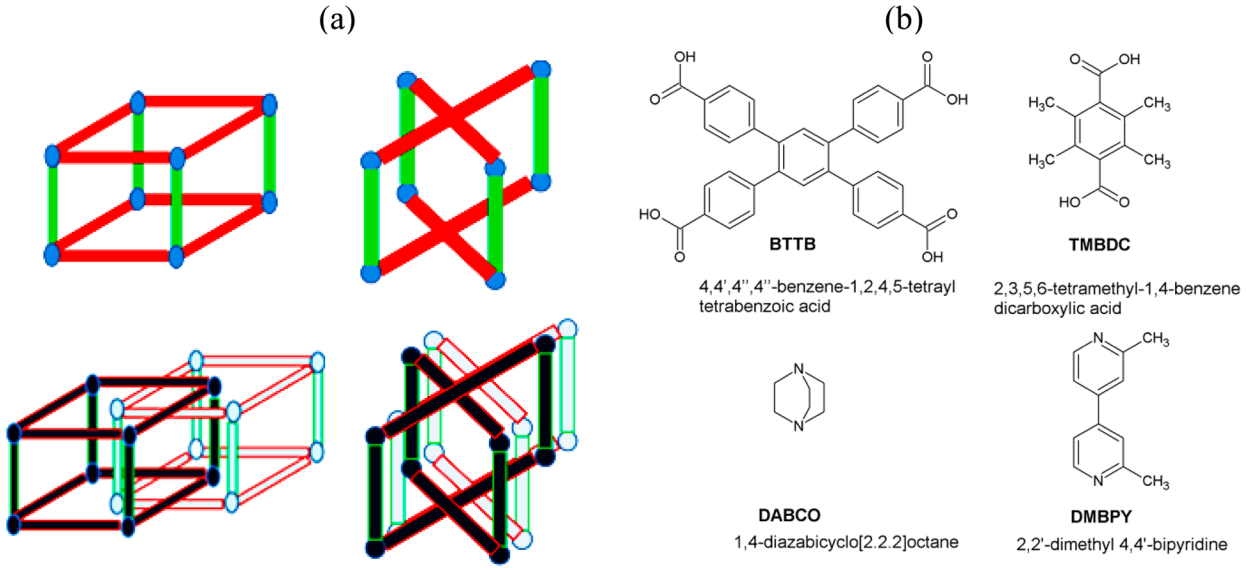

Figure 1. (a) Illustration of noncatenated (top) and 2-fold catenated (bottom) pillared layer metal−organic frameworks synthesized from dicarboxylate (left) and tetracarboxylate ligands (right). The blue corners are the metal nodes, red represents linkage via carboxylate ligands, and green represents linkage via pillar ligands. Black and white represent two different frameworks. (b) Carboxylate (top) and diamine pillar (bottom) ligands used in this work.

under humid conditions due to the low basicity (pK_a) of carboxylate ligands and the low coordination number of their metal centers (only four-coordinated).[16,17,49,50] However, some other carboxylate-ligand-based MOFs, such as UiO-66(Zr),[32] MIL-125(Ti),[27] PCN-56-59(Zr),[45] DUT-51,67-69,[28,46] and MIL-140(Zr),[47] have been reported to be water-stable due to the high oxophilicity and coordination number of their metal centers (eight-coordinated).[16] Similarly, other carboxylate-based MOFs, such as MIL-53(Cr)[21] and MIL-101(Cr),[39] are water-stable, as their metal centers are inert toward water, and hence, now MOF hydrolysis is unfavorable. Imidazolate[30,39] (pK_a ~18.6) and pyrazolate[31,42] (pK_a ~19.8) based MOFs are highly stable under humid or aqueous environments, as the pK_a values of these nitrogen-coordinating ligands are higher than that of water (pK_a ~15.7).

Although the impact of water adsorption and its subsequent effect on the thermodynamic stability of MOF structures could be defined by the acid−base effects of metal centers and ligands, hydrophobicity and ligand sterics are also important in defining the kinetic stability of MOFs, as they can increase the activation energy barrier for the hydrolysis reaction. Ligand functionalization is a promising approach for manipulating the kinetic factors that play a significant role in the stability of the framework. It has been reported earlier that MOF stability in humid environments can be improved by incorporating hydrophobic functional groups,[20,25,29,33−38,43,48] such as alkyl or fluorinated groups, but there is a need to decouple hydrophobicity from steric effects by measuring water adsorption isotherms. Taylor et al.[25] argued that CALF-25 adsorbs appreciable amounts of water, unlike highly hydrophobic fluorous metal−organic frameworks (FMOFs) such as FMOF-1,[29] and is still water resistant, as the nonpolar alkyl functional groups provide steric protection to the metal centers. However, in the majority of the reports,[30−38] water adsorption isotherms have not been measured; e.g., Ma et al.[33] showed that adding methyl groups at the 2,2′-positions on BPY results in a more stable structure (SCUTC-18) than adding methyl groups at the 3,3′-positions (SCUTC-19) without reporting water adsorption isotherms. Hence, it is difficult to conclude whether the MOF is now inherently more stable due to a change in ligand sterics or is stable simply due to the increase in hydrophobicity as a result of functionalization with nonpolar groups. Thus, there is a critical requirement in the MOF field to perform systematic water-stability studies, and water-exposed MOFs should be characterized comprehensively so that we can isolate the specific factors governing structural stability of MOFs and direct the future synthesis efforts toward the construction of new, water-stable MOFs.

The explanation of the MOF degradation mechanisms under humid environments is a very complex problem, because there are various independent factors that play a critical role in the stability of MOFs. To decouple the effects of metal−ligand coordination environment, topology, porosity, metal-type, and ligand-type on the structural stability of MOFs, studies on isostructural series of MOFs are needed in order to systematically study the impact of each specific factor on the MOF water stability by only varying that specific factor. The effect of the metal-type incorporated in MOF systems, such as MOF-74 and DMOF, on the water stability was examined by Liu et al.[26] and Tan et al.,[15] respectively. It was reported that for both MOF systems, the Ni-based variation (Ni-DMOF and Ni-MOF-74) was less vulnerable to hydrolysis. Ni^{2+} has the lowest standard reduction potential among the metals considered in these studies, which makes it less likely for the metal center to react with water.[26] Along the same lines, the water stability of MOF-5 is shown to increase upon doping with Ni^{2+}.[51] We have recently shown that the water-unstable Zn-DMOF structure can be made kinetically stable by functionalizing benzenedicarboxylic acid (BDC) with nonpolar groups, as these groups introduce sterics factors around the metal centers.[18] In other work,[19] we also reported that catenation in pillared MOFs can improve the water resistance of MOFs even when the basicity of the pillar ligand is reduced. Catenation is the interpenetration of two or more identical and independent frameworks (Figure 1a).[7] This catenation can make the ligand

dx.doi.org/10.1021/la503269f | Langmuir 2014, 30, 14300−14307

displacement difficult by locking it in place within the framework.

In this work, we have extended our previous work[18,19,52] by synthesizing new, cobalt-, nickel-, copper-, and zinc-based, water-stable, pillared MOFs of similar topology [Figures S1 (Supporting Information) and 1a] using 2,3,5,6-tetramethyl-1,4-benzenedicarboxylic acid (TMBDC) and 4,4′,4″,4‴-benzene-1,2,4,5-tetrayltetrabenzoic acid (BTTB) as carboxylate ligands and 1,4-diazabicyclo[2.2.2]octane (DABCO) and 2,2′-dimethyl-4,4′-bipyridine (DMBPY) as pillar ligands (Figure 1b). The longer diamine ligand (DMBPY) leads to two-fold catenation [Figures 1a and S1c (Supporting Information)] in the framework. Experiments were performed to measure water adsorption isotherms at 25 °C and 1 bar. PXRD patterns and results from BET modeling[53] of N_2 adsorption isotherms at −196 °C were compared before and after water exposure to determine the impact of water adsorption and its subsequent effect on the stability of MOF structures.

2. EXPERIMENTAL SECTION

2.1. Materials. All the chemicals employed in this work were commercially available and used as-received without further purification from the following sources: Sigma-Aldrich, *N*,*N*-diethylformamide (DEF), *N*,*N*-dimethylformamide (DMF), 4,4′,4″,4‴-benzene-1,2,4,5-tetrayltetrabenzoic acid (BTTB); Chem Service Inc., 2,3,5,6-tetramethyl-1,4-benzenedicarboxylic acid (TMBDC); Acros, 1,4-diazabicyclo[2.2.2]octane (DABCO), ethanol (EtOH); Angene Internationals Ltd, 2,2′-dimethyl-4,4′-bipyridine (DMBPY).

All the new, pillared MOFs reported in this work are summarized in Figure 2 and were synthesized solvothermally. Metal ions and carboxylate ligands form the 2-D sheets, while diamine ligands act as pillars connecting these 2-D sheets in the third dimension [Figures 1a and S1 (Supporting Information)]. Detailed synthesis procedures are summarized below.

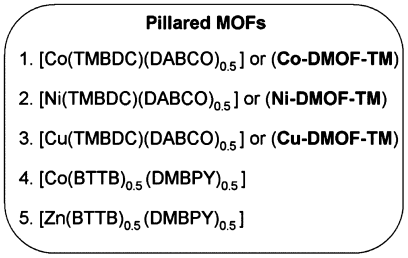

Figure 2. New, water-stable, pillared MOFs synthesized in this work.

2.1.1. M-DMOF-TM (where M = Co, Ni, Cu). M(TMBDC)-$(DABCO)_{0.5}$ or M-DMOF-TM structures were prepared with slight modification from the report of Chun et al.[54] for Zn-DMOF-TM; i.e., 0.63 mmol of metal salt [$Co(NO_3)_2{\cdot}6H_2O$, $Ni(NO_3)_2{\cdot}6H_2O$, $Cu(NO_3)_2{\cdot}3H_2O$], 0.63 mmol of TMBDC ligand, and 0.31 mmol of DABCO ligand were dissolved in 15 mL DMF and left stirring for 3 h at room temperature. The resulting solution was filtered and the filtrate was transferred to a Teflon-lined stainless steel reactor and placed in a preheated oven at 120 °C for 48 h. The solution was then cooled to room temperature in air, and the resulting solid was filtered and repeatedly washed with DMF. Activated samples of M-DMOF-TM were prepared by heating the as-synthesized samples at 110 °C overnight under vacuum.

2.1.2. M-BTTB-DMBPY (where M = Co, Zn). M-$(BTTB)_{0.5}(DMBPY)_{0.5}$ or M-BTTB-DMBPY structures were prepared as suggested by Karra[52] for M-BTTB-BPY; i.e., 0.2 mmol of metal salt [$Co(NO_3)_2{\cdot}6H_2O$, $Zn(NO_3)_2{\cdot}6H_2O$], 0.1 mmol of BTTB ligand, and 0.1 mmol of DMBPY ligand were dissolved in 5 mL of DEF/ethanol/water (2:2:1, v/v). Two drops of 1 N HCl were added to the mixture, and the final mixture was placed in a Teflon-lined stainless steel reactor and placed in a preheated oven at 100 °C for 96 h. The solution was then cooled to room temperature in air, and the resulting solid was filtered and repeatedly washed with DEF. Activated samples were prepared by performing solvent exchange with chloroform and then evacuation overnight under vacuum at 120 °C.

2.2. Characterization. *2.2.1. Single Crystal XRD (X-ray Diffraction).* A Bruker APEX II CCD sealed tube diffractometer with Mo Kα (λ = 0.710 73 Å) radiation and a graphite monochromator was used to collect single crystal X-ray data for Co-BTTB-DMBPY. MOF crystals were mounted on nylon CryoLoops with Paratone-N. The structure was solved by direct methods and refined by full-matrix least-squared techniques using the SHELXTL-97 software suite. Crystallographic details are provided in the Supporting Information (Figure S20, Table S1; CCDC 992483 contains the crystallographic information file).

2.2.2. PXRD (Powder X-ray Diffraction). A X'Pert X-ray PANalytical diffractometer with an X'celerator module and Cu Kα (λ = 1.5418 Å) radiation was used to collect PXRD patterns at room temperature, with a step size of 0.02° in 2θ. The phase purity of the as-synthesized MOF samples was confirmed by comparing PXRD patterns with the simulated patterns from single crystal X-ray diffraction (Figures S3−S7, Supporting Information). To determine the impact of water adsorption and its subsequent effect on the stability of the MOF structures, PXRD patterns of as-synthesized samples were compared with patterns of water-exposed samples and regenerated samples (obtained after activating the water exposed samples).

2.2.3. BET Analysis. A Quadrasorb system from Quantachrome Instruments was used to measure nitrogen adsorption isotherms (Figures S15−S19, Supporting Information) at −196 °C, and the BET model was fitted to these isotherms so that the BET surface areas could be determined for each activated MOF before and after water exposure. Here, the criteria of Walton and Snurr[53] was used to correctly fit the BET model over the low pressure range (P/P_o < 0.05).

2.2.4. Thermogravimetric Analysis. A NETZSCH STA 449 F1 Jupiter device was used to perform thermogravimetric analyses (TGA) of the as-synthesized and activated MOF samples (Figures S8 and S9, Supporting Information) under helium in the temperature range of 30−600 °C with a heating rate of 5 °C/min and flow rate of 20 mL/min.

2.2.5. Fourier Transform Infrared Spectroscopy. Fourier transform infrared (FTIR) spectra of the as-synthesized and activated MOF samples (Figures S10−S14, Supporting Information) were recorded with a PerkinElmer Spectrum One as KBr pellets in the range 400−4000 cm^{-1}. Figures S10−S14 (Supporting Information) confirm the presence of methyl moieties in the frameworks.

2.2.6. Water Vapor Adsorption Isotherms. An Intelligent Gravimetric Analyzer (IGA-3 series, Hiden Isochema) was used to measure water vapor adsorption isotherms at 25 °C and 1 bar. Prior to water adsorption measurements, the samples (~30−40 mg) were activated in situ until no further weight loss was observed. Two mass flow controllers were used to control the relative humidity (RH) by varying the ratio of saturated and dry air. Experiments were conducted only up to 80% or 90% RH so that water condensation did not occur in the equipment. The total gas flow rate was set at 200 cm^3/min for all the experiments, and each adsorption/desorption step was given sufficient time (from 15 min to 20 h) to approach equilibrium for all RH points.

3. RESULTS AND DISCUSSION

3.1. Structure Characterization and Physical Properties. Among the new, pillared MOFs synthesized in this work, we could obtain single crystals only for Co-BTTB-DMBPY (Figure S20, Supporting Information). Analysis of Co-BTTB-DMBPY using single crystal XRD shows that this framework has the same topology as the parent M-BTTB-BPY (where M = Co, Zn and BPY = 4,4′-bipyridine) structure synthesized by Karra.[52] Hence, metal paddle-wheel clusters are connected by

dx.doi.org/10.1021/la503269f | Langmuir 2014, 30, 14300−14307

Table 1. Comparison of Properties of Water-Stable, Pillared MOFs Synthesized in this Work

MOF	pore size (Å)	pore volume[a] (cm^3/g)	BET surface area[d] (m^2/g)	activation process (under vacuum)	thermal stability (°C)	features	BET surface area,[d] after 80% or 90% RH
Co-DMOF-TM	~3.5[b]	0.488	1052	110 °C (1 h)	310	noncatenated	1016
Ni-DMOF-TM	~3.5[b]	0.484	1095	110 °C (2 h)	310	noncatenated	1068
Cu-DMOF-TM	~3.5[b]	0.461	1041	110 °C (1 h)	310	noncatenated	990
Co-BTTB-DMBPY	4.41[c]	0.290	809	chloroform exchange and 120 °C (12 h)	340	2-fold catenated	807
Zn-BTTB-DMBPY	~4.41	0.269	749	chloroform exchange and 120 °C (12 h)	340	2-fold catenated	740

[a]Obtained from the Dubinin−Astakov model of N_2 adsorption at 77 K. [b]Based on the 3.5 Å pore size of Zn-DMOF-TM.[54] [c]Calculated using the approach of Haldoupis et al.[56] [d]BET analysis.[53]

BTTB ligands to form 2-D layers that are further pillared together by DMBPY ligands, giving rise to a porous 3D framework (CCDC 992483 contains the CIF). Two identical and independent 3D frameworks interpenetrate [Figures 1b and S1c (Supporting Information)] with each other, forming the 2-fold catenated final structure of this series of MOFs. However, DABCO-based, pillared MOFs M-DMOF-TM (where M = Co, Ni, Cu) are noncatenated, similar to the parent Zn-DMOF-TM structure.[54] Since we could obtain a single-crystal structure only for Co-BTTB-DMBPY, we used the simulated patterns of the isostructural pillared MOFs Zn-BTTB-BPY[52] and Zn-DMOF-TM[54] for Zn-BTTB-DMBPY and M-DMOF-TM (where M = Co, Ni, Cu), respectively. PXRD patterns of the as-synthesized M-DMOF-TM MOFs confirm that these materials are isostructural to the parent Zn-DMOF-TM structure (Figure S2, Supporting Information). As expected, N_2 adsorption measurements (Figures S15−S19, Supporting Information) at −196 °C on the activated MOF samples showed typical type I behavior according to the IUPAC classification.[3] Furthermore, we observe that methyl functionalization leads to a reduction in porosity (Table 1) for M-BTTB-DMBPY (where M = Co, Zn) compared to the parent M-BTTB-BPY (where M = Co, Zn),[52] whereas M-DMOF-TM (where M = Co, Ni, Cu) shows porosity similar to the parent Zn-DMOF-TM.[28] TGA analyses of M-DMOF-TM samples show that they all decompose around 310 °C [Figure S8 (Supporting Information), Table 1], similar to the parent Zn-DMOF-TM material.[54] However, M-BTTB-DMBPY decomposes at a slightly higher temperature of 340 °C [Figure S9 (Supporting Information), Table 1], since catenated crystal structures display higher thermal stability.[55] FTIR spectra (Figures S10−S14, Supporting Information) for as-synthesized M-DMOF-TM and M-BTTB-DMBPY show peaks around 1680 and 3000 cm^{-1}, corresponding to the stretching frequency of C═O bond in DMF/DEF and C−H bond in the methyl moieties attached to the benzene rings, respectively. Upon activation the peak at 1680 cm^{-1} disappears, whereas the peaks near 3000 cm^{-1} are retained. Hence, FTIR spectra (Figures S10−S14, Supporting Information) of pillared MOFs synthesized in this work confirm the presence of methyl moieties in the framework.

3.2. Structural Stability Analysis under Humid Environments. The stability of M-DMOF-TM (where M = Co, Ni, Cu) and M-BTTB-DMBPY (where M = Co, Zn) after water exposure (80% or 90% RH) was evaluated using water vapor adsorption isotherms along with PXRD patterns and results from BET modeling[53] of N_2 adsorption isotherms before and after water exposure. Figure 3 compares the water vapor adsorption behavior at 25 °C and 1 bar for M-DMOF-TM with that of the parent Zn-DMOF-TM structure. All of

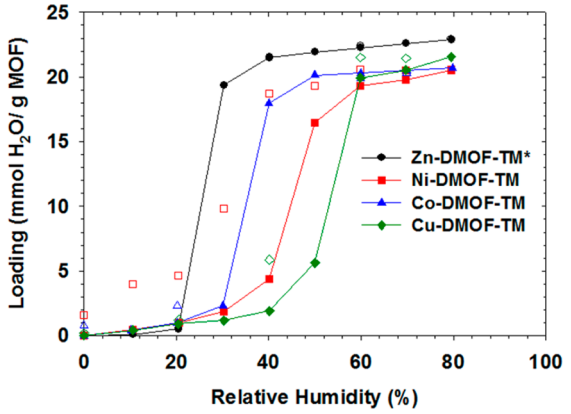

Figure 3. Water vapor adsorption isotherms at 25 °C for desolvated compounds of M-DMOF-TM (closed symbols, adsorption; open symbols, desorption). Lines connecting the adsorption points are to faciliate viewing. *Reported from our previous work.[18]

these DABCO-based, noncatenated, pillared MOFs display type V behavior[57] similar to traditional porous materials, such as BPL carbon, SBA-15, and MCM-41.[17] Unlike the parent Zn-DMOF-TM, the Co-, Ni-, and Cu-based variations of DMOF-TM show varying levels of hysteresis and retain some amount of water, even when the stream is switched to dry air (0% RH point in the desorption curve). This is unexpected because in these DABCO-based, pillared MOFs there are no unsaturated metal sites available for water to interact with. Recently, Wu et al.[58] showed that framework defects can have significant impact on adsorption properties of MOFs, and Canivet et al.[59] suggested that hysteresis in water adsorption isotherms of MOFs can be accredited to framework flexibility. It is possible that the M-DMOF-TM (where M = Co, Ni, Cu, and Zn) structures also have varying levels of flexibility or defects that create local heterogeneity in the framework and explain the differing water adsorption and desorption behavior. Therefore, the pore-filling step in these MOFs occurs at a different RH point, even when their pore sizes are very similar. Typically, the pore-filling step occurs first (at the lowest levels of RH) for the smallest pore material and last for the largest pore material.[17]

M-DMOF-TM (where M = Co, Ni, Cu) displayed no change in crystallinity (Figure 4) or loss of surface area (Table 1) after exposure to humid conditions similar to the parent Zn-DMOF-TM material, as shown in our previous work.[18,19] The water vapor adsorption capacities at 80% RH are 20.7 mmol/g (37.2 wt %) for Co-DMOF-TM, 20.5 mmol/g (36.9 wt %) for Ni-DMOF-TM, 21.5 mmol/g (38.8 wt %) for Cu-DMOF-TM, and 22.9 mmol/g (41.2 wt %) for Zn-DMOF-TM. The Co-, Ni-, Cu-, and Zn-based variations of the unfunctionalized

dx.doi.org/10.1021/la503269f | Langmuir 2014, 30, 14300−14307

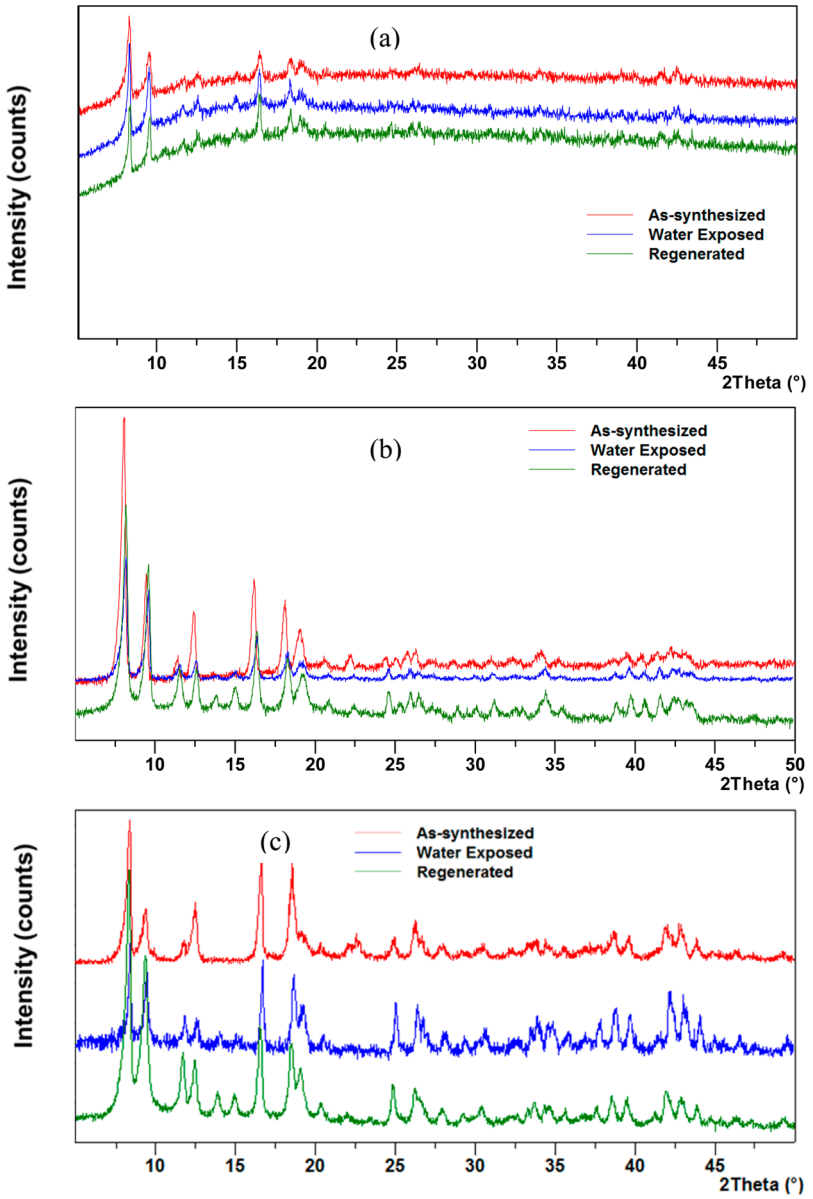

Figure 4. PXRD patterns for as-synthesized, water-exposed (after 80% RH), and regenerated (a) Co-DMOF-TM, (b) Ni-DMOF-TM, and (c) Cu-DMOF-TM.

DMOF structure have been shown to collapse under 60% RH.[15,17,40] However, methyl groups grafted on the BDC ligand in DMOF-TM introduce sterics factors around the metal centers.[18,19] Hence, Co-, Ni-, Cu-, and Zn-based, tetramethyl-functionalized variations of DMOF (DMOF-TM) are remarkably stable, even when they have very high water vapor adsorption loadings (>20 mmol/g at 80% RH). Only a few MOFs, such as UiO-66, MIL-100(Fe), and MIL-101(Cr), display such stability after adsorbing large amounts of water.[17,39,24]

Figure 5 shows the water vapor adsorption isotherms at 25 °C and 1 bar for the BTTB-ligand-based, 2-fold catenated, pillared MOFs. Up to 70% RH, all of these isostructural, pillared MOFs display type VII behavior,[57] similar to MOF-508,[19] and hence, these materials are very hydrophobic. However, at higher RH, the pore-filling step occurs differently in these MOFs. Furthermore, the desorption branch in their isotherms shows varying levels of hysteresis and shows retention of varying amounts of water at the 0% RH point in the desorption curve. This is unexpected, because these BTTB-ligand-based, 2-fold catenated, pillared MOFs are isostructural and have very similar pores. Most likely, along the same lines of M-DMOF-TM (where M = Co, Ni, Cu, and Zn, Figure 3), these BTTB-ligand-based MOFs also have varying levels of flexibility or defects, which impact their water adsorption.

These BTTB-DMBPY-based, catenated, pillared MOFs are stable even after exposure to 90% RH, as there is negligible change in their surface area and crystallinity (Table 1, Figure 6) similar to the parent BTTB-BPY-based, pillared MOFs.[52] However, noncatenated, pillared MOFs such as DMOF collapse under 60% RH,[15,17,40] even when it is synthesized with the DABCO pillar ligand, which is much more basic than the BPY and DMBPY pillar ligands (Table 2). It should be noted that the pK_a value of BTTB (Table 2) is very similar to that of the BDC ligand (pK_a ~ 3.73)[60] used for the synthesis of DMOF, and catenated structures are expected to be more stable.[55] Hence, the stability of these BTTB-based, pillared MOFs could be attributed to catenation present in their

dx.doi.org/10.1021/la503269f | *Langmuir* 2014, 30, 14300−14307

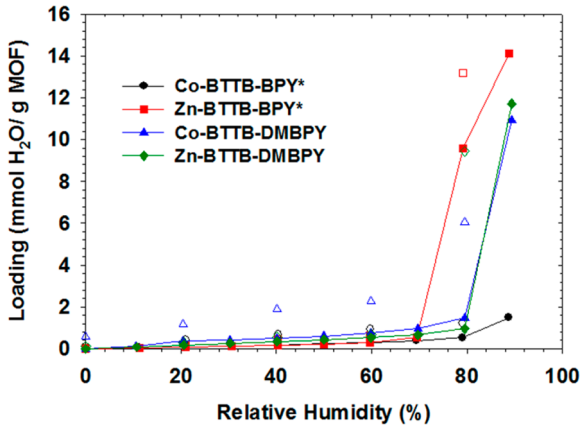

Figure 5. Water vapor adsorption isotherms at 25 °C for desolvated compounds of M-BTTB-DMBPY and M-BTTB-BPY (closed symbols, adsorption; open symbols, desorption). Lines connecting the adsorption points are to faciliate viewing. *Reported in our previous work.[52]

frameworks, similar to MOF-508, which has been reported[19] to be stable, too, after 90% RH exposure, even when the basicity of the pillar ligand is low (Table 2). Catenation could make the ligand displacement difficult by locking it in place within the framework.

4. CONCLUSION

In our previous reports, we have shown that structural factors such as ligand sterics and catenation can enhance MOF stability under humid conditions. In this work, we have used these structural factors to synthesize cobalt-, nickel-, copper-, and zinc-based, new, water-stable, pillared MOFs of similar topologies. Our study shows that, unlike the parent DMOF structure, which collapses under 60% RH, tetramethyl-functionalized variations or DMOF-TM are remarkably stable, even when they have very high water vapor adsorption loadings (> 20 mmol/g at 80% RH). These methyl groups grafted on the BDC ligand introduce steric factors around the metal centers. BTTB-based, pillared MOFs are synthesized with bipyridyl-based, pillar ligands, which have lower basicity than DABCO but are still stable after exposure to 90% RH due to the presence of catenation in their frameworks, similar to MOF-508, which also has been reported to be stable after 90% RH exposure. The results of this work show that by incorporating specific factors governing structural stability into the framework, it is possible to synthesize more water stable MOFs.

Table 2. Comparison of pK_a Values[60] of Ligands Used in the Synthesis of Pillared MOFs

MOF	ligand	pK_a
M-DMOF-TM	TMBDC, DABCO	3.80, 8.86
M-BTTB-DMBPY	BTTB, DMBPY	4.01, 5.60
M-BTTB-BPY	BTTB, BPY	4.01, 4.60

■ ASSOCIATED CONTENT

Supporting Information

3D structures of MOFs, PXRD patterns, TGA curves, FTIR spectra, crystallographic data, and N_2 adsorption data. This material is available free of charge via the Internet at http://pubs.acs.org.

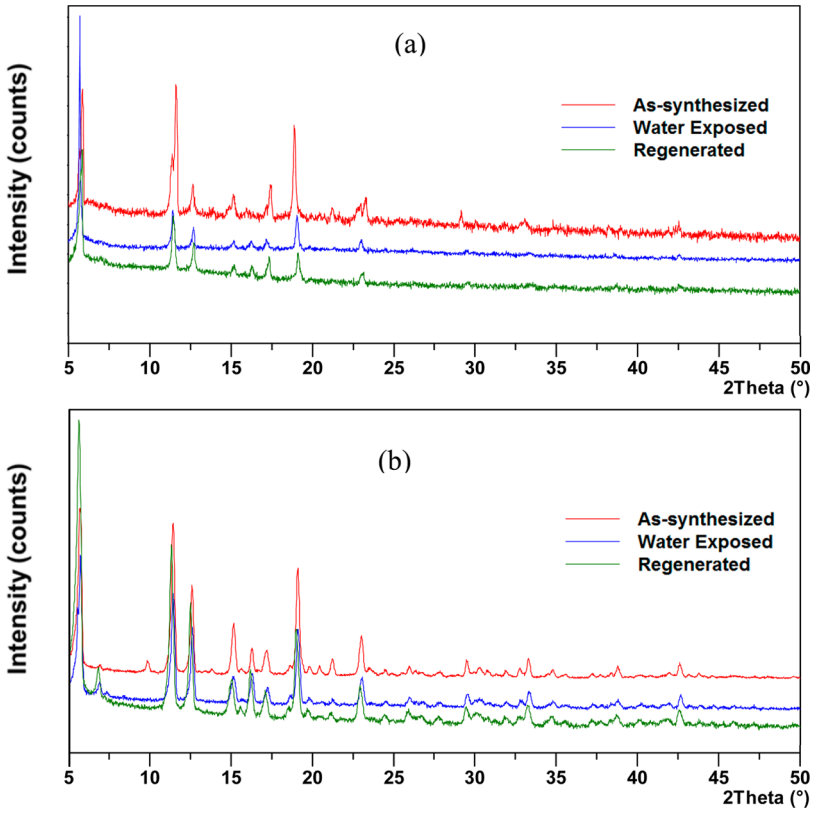

Figure 6. PXRD patterns for as-synthesized, water-exposed (after 90% RH), and regenerated (a) Co-BTTB-DMBPY and (b) Zn-BTTB-DMBPY.

dx.doi.org/10.1021/la503269f | Langmuir 2014, 30, 14300−14307

AUTHOR INFORMATION

Corresponding Author

*E-mail: krista.walton@chbe.gatech.edu. Fax: +1-404-894-2866. Tel: +1-404-894-5254.

Notes

The authors declare no competing financial interest.

ACKNOWLEDGMENTS

This material is based upon work supported by Army Research Office PECASE Award W911NF-10-1-0079 and Contract W911NF-10-1-0076.

REFERENCES

(1) Ferey, G. Some Suggested Perspectives for Multifunctional Hybrid Porous Solids. *Dalton Trans.* **2009**, *23*, 4400−4415.

(2) Kuppler, R. J.; Timmons, D. J.; Fang, Q. R.; Li, J. R.; Makal, T. A.; Young, M. D.; Yuan, D. Q.; Zhao, D.; Zhuang, W. J.; Zhou, H. C. Potential Applications of Metal−Organic Frameworks. *Coord. Chem. Rev.* **2009**, *253* (23−24), 3042−3066.

(3) Kitagawa, S.; Kitaura, R.; Noro, S. Functional Porous Coordination Polymers. *Angew. Chem., Int. Ed.* **2004**, *43* (18), 2334−2375.

(4) Rowsell, J. L.; Yaghi, O. M. Effects of Functionalization, Catenation, and Variation of the Metal Oxide and Organic Linking Units on the Low-Pressure Hydrogen Adsorption Properties of Metal−Organic Frameworks. *J. Am. Chem. Soc.* **2006**, *128* (4), 1304−1315.

(5) Farha, O. K.; Hupp, J. T. Rational Design, Synthesis, Purification, and Activation of Metal−Organic Framework Materials. *Acc. Chem. Res.* **2010**, *43* (8), 1166−1175.

(6) Eddaoudi, M.; Kim, J.; Rosi, N.; Vodak, D.; Wachter, J.; O'Keeffe, M.; Yaghi, O. M. Systematic Design of Pore Size and Functionality in Isoreticular MOFs and Their Application in Methane Storage. *Science* **2002**, *295* (5554), 469−472.

(7) Czaja, A. U.; Trukhan, N.; Muller, U. Industrial Applications of Metal−Organic Frameworks. *Chem. Soc. Rev.* **2009**, *38* (5), 1284−1293.

(8) Li, J. R.; Kuppler, R. J.; Zhou, H. C. Selective Gas Adsorption and Separation in Metal−Organic Frameworks. *Chem. Soc. Rev.* **2009**, *38* (5), 1477−1504.

(9) Caskey, S. R.; Wong-Foy, A. G.; Matzger, A. J. Dramatic Tuning of Carbon Dioxide Uptake Via Metal Substitution in a Coordination Polymer with Cylindrical Pores. *J. Am. Chem. Soc.* **2008**, *130* (33), 10870−10871.

(10) Sumida, K.; Rogow, D. L.; Mason, J. A.; McDonald, T. M.; Bloch, E. D.; Herm, Z. R.; Bae, T. H.; Long, J. R. Carbon Dioxide Capture in Metal−Organic Frameworks. *Chem. Rev.* **2012**, *112* (2), 724−781.

(11) Tanabe, K. K.; Cohen, S. M. Postsynthetic Modification of Metal−Organic Frameworks—A Progress Report. *Chem. Soc. Rev.* **2011**, *40* (2), 498−519.

(12) Burtch, N. C.; Jasuja, H.; Walton, K. S. Water Stability and Adsorption in Metal−Organic Frameworks. *Chem. Rev.* **2014**, *114*, 10575−10612.

(13) DeCoste, J. B.; Peterson, G. W.; Jasuja, H.; Glover, T. G.; Huang, Y. G.; Walton, K. S. Stability and Degradation Mechanisms of Metal−Organic Frameworks Containing the $Zr_6O_4(OH)_4$ Secondary Building Unit. *J. Mater. Chem. A* **2013**, *1* (18), 5642−5650.

(14) DeCoste, J. B.; Peterson, G. W.; Schindler, B. J.; Killops, K. L.; Browe, M. A.; Mahle, J. J. The Effect of Water Adsorption on the Structure of the Carboxylate Containing Metal−Organic Frameworks Cu-BTC, Mg-MOF-74, and UiO-66. *J. Mater. Chem. A* **2013**, *1* (38), 11922−11932.

(15) Tan, K.; Nijem, N.; Canepa, P.; Gong, Q.; Li, J.; Thonhauser, T.; Chabal, Y. J. Stability and Hydrolyzation of Metal Organic Frameworks with Paddle-Wheel SBUs upon Hydration. *Chem. Mater.* **2012**, *24* (16), 3153−3167.

(16) Low, J. J.; Benin, A. I.; Jakubczak, P.; Abrahamian, J. F.; Faheem, S. A.; Willis, R. R. Virtual High Throughput Screening Confirmed Experimentally: Porous Coordination Polymer Hydration. *J. Am. Chem. Soc.* **2009**, *131* (43), 15834−15842.

(17) Schoenecker, P. M.; Carson, C. G.; Jasuja, H.; Flemming, C. J. J.; Walton, K. S. Effect of Water Adsorption on Retention of Structure and Surface Area of Metal−Organic Frameworks. *Ind. Eng. Chem. Res.* **2012**, *51* (18), 6513−6519.

(18) Jasuja, H.; Burtch, N. C.; Huang, Y. G.; Cai, Y.; Walton, K. S. Kinetic Water Stability of an Isostructural Family of Zinc-Based Pillared Metal−Organic Frameworks. *Langmuir* **2013**, *29* (2), 633−642.

(19) Jasuja, H.; Walton, K. S. Effect of Catenation and Basicity of Pillared Ligands on the Water Stability of MOFs. *Dalton Trans.* **2013**, *42* (43), 15421−15426.

(20) Decoste, J. B.; Peterson, G. W.; Smith, M. W.; Stone, C. A.; Willis, C. R. Enhanced Stability of Cu-BTC MOF via Perfluorohexane Plasma-Enhanced Chemical Vapor Deposition. *J. Am. Chem. Soc.* **2012**, *134* (3), 1486−1489.

(21) Kang, I. J.; Khan, N. A.; Haque, E.; Jhung, S. H. Chemical and Thermal Stability of Isotypic Metal−Organic Frameworks: Effect of Metal Ions. *Chemistry* **2011**, *17* (23), 6437−6442.

(22) Bellarosa, L.; Calero, S.; Lopez, N. Early Stages in the Degradation of Metal−Organic Frameworks in Liquid Water from First-Principles Molecular Dynamics. *Phys. Chem. Chem. Phys.* **2012**, *14* (20), 7240−7245.

(23) Han, S. S.; Choi, S. H.; van Duin, A. C. Molecular Dynamics Simulations of Stability of Metal−Organic Frameworks against H_2O using the ReaxFF Reactive Force Field. *Chem. Commun. (Cambridge, U. K.)* **2010**, *46* (31), 5713−5715.

(24) Soubeyrand-Lenoir, E.; Vagner, C.; Yoon, J. W.; Bazin, P.; Ragon, F.; Hwang, Y. K.; Serre, C.; Chang, J. S.; Llewellyn, P. L. How Water Fosters a Remarkable 5-Fold Increase in Low-Pressure CO_2 Uptake within Mesoporous MIL-100(Fe). *J. Am. Chem. Soc.* **2012**, *134* (24), 10174−10181.

(25) Taylor, J. M.; Vaidhyanathan, R.; Iremonger, S. S.; Shimizu, G. K. Enhancing Water Stability of Metal−Organic Frameworks via Phosphonate Monoester Linkers. *J. Am. Chem. Soc.* **2012**, *134* (35), 14338−14340.

(26) Liu, J.; Benin, A. I.; Furtado, A. M.; Jakubczak, P.; Willis, R. R.; LeVan, M. D. Stability Effects on CO_2 Adsorption for the DOBDC Series of Metal−Organic Frameworks. *Langmuir* **2011**, *27* (18), 11451−11456.

(27) Jeremias, F.; Lozan, V.; Henninger, S. K.; Janiak, C. Programming MOFs for Water Sorption: Amino-Functionalized MIL-125 and UiO-66 for Heat Transformation and Heat Storage Applications. *Dalton Trans.* **2013**, *42*, 15967−15973.

(28) Bon, V.; Senkovskyy, V.; Senkovska, I.; Kaskel, S. Zr(IV) and Hf(IV) Based Metal−Organic Frameworks with reo-Topology. *Chem. Commun.* **2012**, *48* (67), 8407−8409.

(29) Yang, C.; Kaipa, U.; Mather, Q. Z.; Wang, X.; Nesterov, V.; Venero, A. F.; Omary, M. A. Fluorous Metal−Organic Frameworks with Superior Adsorption and Hydrophobic Properties toward Oil Spill Cleanup and Hydrocarbon Storage. *J. Am. Chem. Soc.* **2011**, *133* (45), 18094−18097.

(30) Cychosz, K. A.; Matzger, A. J. Water Stability of Microporous Coordination Polymers and the Adsorption of Pharmaceuticals from Water. *Langmuir* **2010**, *26* (22), 17198−17202.

(31) Choi, H. J.; Dinca, M.; Dailly, A.; Long, J. R. Hydrogen Storage in Water-Stable Metal−Organic Frameworks Incorporating 1,3- and 1,4-Benzenedipyrazolate. *Energy Env. Sci.* **2010**, *3* (1), 117−123.

(32) Cavka, J. H.; Jakobsen, S.; Olsbye, U.; Guillou, N.; Lamberti, C.; Bordiga, S.; Lillerud, K. P. A New Zirconium Inorganic Building Brick Forming Metal Organic Frameworks with Exceptional Stability. *J. Am. Chem. Soc.* **2008**, *130* (42), 13850−13851.

(33) Ma, D.; Li, Y.; Li, Z. Tuning the Moisture Stability of Metal−Organic Frameworks by Incorporating Hydrophobic Functional Groups at Different Positions of Ligands. *Chem. Commun. (Cambridge, U. K.)* **2011**, *47* (26), 7377−7379.

(34) Yang, J.; Grzech, A.; Mulder, F. M.; Dingemans, T. J. Methyl Modified MOF-5: A Water Stable Hydrogen Storage Material. *Chem. Commun. (Cambridge, U. K.)* **2011**, *47* (18), 5244−5246.
(35) Nguyen, J. G.; Cohen, S. M. Moisture-Resistant and Superhydrophobic Metal−Organic Frameworks Obtained via Post-synthetic Modification. *J. Am. Chem. Soc.* **2010**, *132* (13), 4560−4561.
(36) Li, T.; Chen, D.-L.; Sullivan, J. E.; Kozlowski, M. T.; Johnson, J. K.; Rosi, N. L. Systematic modulation and enhancement of CO_2: N_2 Selectivity and Water Stability in an Isoreticular Series of Bio-MOF-11 Analogues. *Chem. Sci.* **2013**, *4* (4), 1746−1755.
(37) Makal, T. A.; Wang, X.; Zhou, H.-C. Tuning the Moisture and Thermal Stability of Metal−Organic Frameworks through Incorporation of Pendant Hydrophobic Groups. *Cryst. Growth Des.* **2013**, *13* (11), 4760−4768.
(38) Liu, H.; Zhao, Y.; Zhang, Z.; Nijem, N.; Chabal, Y. J.; Peng, X.; Zeng, H.; Li, J. Ligand Functionalization and Its Effect on CO_2 Adsorption in Microporous Metal−Organic Frameworks. *Chem.—Asian J.* **2013**, *8* (4), 778−785.
(39) Kusgens, P.; Rose, M.; Senkovska, I.; Frode, H.; Henschel, A.; Siegle, S.; Kaskel, S. Characterization of Metal−Organic Frameworks by Water Adsorption. *Microporous Mesoporous Mater.* **2009**, *120* (3), 325−330.
(40) Liang, Z. J.; Marshall, M.; Chaffee, A. L. CO_2 Adsorption, Selectivity and Water Tolerance of Pillared-Layer Metal Organic Frameworks. *Microporous Mesoporous Mater.* **2010**, *132* (3), 305−310.
(41) Kaye, S. S.; Dailly, A.; Yaghi, O. M.; Long, J. R. Impact of Preparation and Handling on the Hydrogen Storage Properties of Zn_4O(1,4-benzenedicarboxylate)$_3$ (MOF-5). *J. Am. Chem. Soc.* **2007**, *129* (46), 14176−14177.
(42) Colombo, V.; Galli, S.; Choi, H. J.; Han, G. D.; Maspero, A.; Palmisano, G.; Masciocchi, N.; Long, J. R. High Thermal and Chemical Stability in Pyrazolate-Bridged Metal−Organic Frameworks with Exposed Metal Sites. *Chem. Sci.* **2011**, *2* (7), 1311−1319.
(43) Wu, T.; Shen, L.; Luebbers, M.; Hu, C.; Chen, Q.; Ni, Z.; Masel, R. I. Enhancing the Stability of Metal−Organic Frameworks in Humid Air by Incorporating Water Repellent Functional Groups. *Chem. Commun. (Cambridge, U. K.)* **2010**, *46* (33), 6120−6122.
(44) Liu, H.; Zhao, Y. G.; Zhang, Z. J.; Nijem, N.; Chabal, Y. J.; Zeng, H. P.; Li, J. The Effect of Methyl Functionalization on Microporous Metal−Organic Frameworks' Capacity and Binding Energy for Carbon Dioxide Adsorption. *Adv. Funct. Mater.* **2011**, *21* (24), 4754−4762.
(45) Jiang, H.-L.; Feng, D.; Liu, T.-F.; Li, J.-R.; Zhou, H.-C. Pore Surface Engineering with Controlled Loadings of Functional Groups via Click Chemistry in Highly Stable Metal−Organic Frameworks. *J. Am. Chem. Soc.* **2012**, *134* (36), 14690−14693.
(46) Bon, V.; Senkovska, I.; Baburin, I. A.; Kaskel, S. Zr- and Hf-Based Metal−Organic Frameworks: Tracking Down the Polymorphism. *Cryst. Growth Des.* **2013**, *13* (3), 1231−1237.
(47) Guillerm, V.; Ragon, F.; Dan-Hardi, M.; Devic, T.; Vishnuvarthan, M.; Campo, B.; Vimont, A.; Clet, G.; Yang, Q.; Maurin, G.; Ferey, G.; Vittadini, A.; Gross, S.; Serre, C. A Series of Isoreticular, Highly Stable, Porous Zirconium Oxide Based Metal−Organic Frameworks. *Angew. Chem., Int. Ed.* **2012**, *51* (37), 9267−9271.
(48) Chen, T.-H.; Popov, I.; Zenasni, O.; Daugulis, O.; Miljanic, O. S. Superhydrophobic Perfluorinated Metal−Organic Frameworks. *Chem. Commun.* **2013**, *49* (61), 6846−6848.
(49) Greathouse, J. A.; Allendorf, M. D. The Interaction of Water with MOF-5 Simulated by Molecular Dynamics. *J. Am. Chem. Soc.* **2006**, *128* (33), 10678−10679.
(50) Li, Y.; Yang, R. T. Gas Adsorption and Storage in Metal−Organic Framework MOF-177. *Langmuir* **2007**, *23* (26), 12937−12944.
(51) Li, H.; Shi, W.; Zhao, K.; Li, H.; Bing, Y.; Cheng, P. Enhanced Hydrostability in Ni-Doped MOF-5. *Inorg. Chem.* **2012**, *51* (17), 9200−9207.
(52) Karra, J. *Development of Porous Metal Organic Frameworks for Gas Adsorption Applications*; Georgia Institute of Technology: Atlanta, GA, 2011.
(53) Walton, K. S.; Snurr, R. Q. Applicability of the BET Method for Determining Surface Areas of Microporous Metal−Organic Frameworks. *J. Am. Chem. Soc.* **2007**, *129* (27), 8552−8556.
(54) Chun, H.; Dybtsev, D. N.; Kim, H.; Kim, K. Synthesis, X-ray Crystal Structures, and Gas Sorption Properties of Pillared Square Grid Nets based on Paddle-Wheel Motifs: Implications for Hydrogen Storage in Porous Materials. *Chemistry* **2005**, *11* (12), 3521−3529.
(55) Zhang, J.; Wojtas, L.; Larsen, R. W.; Eddaoudi, M.; Zaworotko, M. J. Temperature and Concentration Control over Interpenetration in a Metal−Organic Material. *J. Am. Chem. Soc.* **2009**, *131* (47), 17040−17041.
(56) Haldoupis, E.; Nair, S.; Sholl, D. S. Efficient Calculation of Diffusion Limitations in Metal Organic Framework Materials: A Tool for Identifying Materials for Kinetic Separations. *J. Am. Chem. Soc.* **2010**, *132* (21), 7528−7539.
(57) Ng, E. P.; Mintova, S. Nanoporous Materials with Enhanced Hydrophilicity and High Water Sorption Capacity. *Microporous Mesoporous Mater.* **2008**, *114* (1-3), 1−26.
(58) Wu, H.; Chua, Y. S.; Krungleviciute, V.; Tyagi, M.; Chen, P.; Yildirim, T.; Zhou, W. Unusual and Highly Tunable Missing-Linker Defects in Zirconium Metal−Organic Framework UiO-66 and their Important Effects on Gas Adsorption. *J. Am. Chem. Soc.* **2013**, *135* (28), 10525−10532.
(59) Canivet, J.; Bonnefoy, J.; Daniel, C.; Legrand, A.; Coasne, B.; Farrusseng, D. Structure−Property Relationships of Water Adsorption in Metal−Organic Frameworks. *New J. Chem.* **2014**, *38*, 3102−3111.
(60) Hilal, S.; Karickhoff, S. W.; Carreira, L. A. A Rigorous Test for SPARC's Chemical Reactivity Models: Estimation of More than 4300 Ionization pKa's. *Quant. Struct.-Act. Relat.* **1995**, *14*, 348.